Light Z' signatures at the LHC

Yaşar Hiçyılmaz,[1,2,*] Shaaban Khalil,[3,†] and Stefano Moretti[2,4,‡,§]

[1]*Department of Physics, Balıkesir University, TR10145, Balıkesir, Turkey*
[2]*School of Physics and Astronomy, University of Southampton, Highfield, Southampton SO17 1BJ, United Kingdom*
[3]*Center for Fundamental Physics, Zewail City of Science and Technology, 6 October City, Giza 12588, Egypt*
[4]*Department of Physics and Astronomy, Uppsala University, Box 516, SE-751 20 Uppsala, Sweden*

(Received 30 September 2022; accepted 6 February 2023; published 27 February 2023)

In this work, we discuss a distinctive $pp \to \text{Higgs} \to Z'Z' \to 4l$ ($l = e, \mu$) signal at the LHC, where the "Higgs" label refers to the Standard Model–like Higgs state discovered in 2012 or a lighter one in the framework of a theoretical model embedding a spontaneously broken $U(1)'$ symmetry in addition to the Standard Model gauge group. The additional $U(1)'$ symmetry generates a very light Z' state, with both vector and axial (nonuniversal) couplings to fermions, which are able to explain the so-called Atomki anomaly, compliant with current measurements of the anomalous magnetic moments of electron and muon as well as beam dump experiments. We show that the cross section for this process should be sufficiently large to afford one with significant sensitivity during run 3 of the LHC.

DOI: 10.1103/PhysRevD.107.035030

I. INTRODUCTION

A light neutral Z' boson (often dubbed a "dark photon"), with mass of order 17 MeV, provides a natural explanation for the clear anomaly observed by the Atomki collaboration [1] in the decay of excited states of Beryllium [2–7]. Furthermore, several studies have been conducted to investigate the effects of such light Z' on the anomalous magnetic moments (AMMs) of the electron (a_e) and muon (a_μ) as well as B anomalies such as $R_{K^{(*)}}$ [8–17].

In this paper we analyze some LHC signatures of a light Z' associated with a nonuniversal $U(1)'$ extension of the Standard Model (SM). This type of scenario has been shown to account for both the Atomki anomaly and $a_{e,\mu}$ results [18]. In addition, we revisit the contributions of such light Z' to these observables to see how the most recent experimental results constrain the associated couplings.

We focus on a nonuniversal $U(1)'$ extension of the SM in which the kinetic term in the Lagrangian is given by

$$\mathcal{L}_{\text{kin}} = -\frac{1}{4}\hat{F}_{\mu\nu}\hat{F}^{\mu\nu} - \frac{1}{4}\hat{F}'_{\mu\nu}\hat{F}'^{\mu\nu} - \frac{\eta}{2}\hat{F}'_{\mu\nu}\hat{F}^{\mu\nu}, \tag{1}$$

where η quantifies the mixing between the SM $U(1)_Y$ and extra $U(1)'$. After the diagonalization of Eq. (1), the covariant derivative can be written as

$$\mathcal{D}_\mu = \partial_\mu + \cdots + ig_1 Y B_\mu + i(\tilde{g}Y + g'z)B'_\mu, \tag{2}$$

where Y and g_1 are the hypercharge and its gauge coupling while z and g' are the $U(1)'$ charge and its gauge coupling. Further, $\tilde{g}$ is the mixed gauge coupling between the two groups. The $U(1)'$ symmetry is broken by a new SM singlet scalar, χ, with $U(1)'$ charge z_χ and vacuum expectation value v'. The scalar potential for the Higgs fields can be written as

$$V(H,\chi) = -\mu^2|H|^2 + \lambda|H|^4 - \mu_\chi^2|\chi|^2 + \lambda_\chi|\chi|^4 + \kappa|\chi|^2|H|^2. \tag{3}$$

Here, H is the SM Higgs doublet while κ is the mixing parameter which connects that SM and χ Higgs fields. After electroweak symmetry breaking, for $\mu^2 = \lambda v^2 + \frac{1}{2}\kappa v'^2$ and $\mu_\chi^2 = \lambda_\chi v'^2 + \frac{1}{2}\kappa v^2$, the Higgs mass matrix in the (h_2, h_1) basis can be written as

$$m^2_{h_2 h_1} = \begin{pmatrix} 2\lambda v^2 & \kappa v v' \\ \kappa v v' & 2\lambda_\chi v'^2 \end{pmatrix}, \tag{4}$$

*Y.Hicyilmaz@soton.ac.uk
†skhalil@zewailcity.edu.eg
‡S.Moretti@soton.ac.uk
§Stefano.Moretti@physics.uu.se

where h_2 is dominantly the SM-like Higgs boson while the exotic state h_1 is dominantly the singlet Higgs (χ-like). In this work, we consider $m_{h_1} < m_{h_2}$ and the $h_1 \to Z'Z'$ branching ratio ≥ 0.95, which are be compatible with experimental results. The SM-like Higgs boson h_2 can decay to Z' pairs too, proportionally to κ. Moreover, the spontaneous breaking of the $U(1)'$ symmetry implies the existence of a mass term $m_{Z'} = g' z_\chi v'$. Thus, if $g' \sim \mathcal{O}(10^{-4} - 10^{-5})$, M'_Z would be of order $\mathcal{O}(10)$ MeV. It is worth noting that we adopt nonuniversal charge assignments of the SM particles under $U(1)'$, as discussed in Ref. [18]. These assignments satisfy anomaly cancellation conditions, enforcing a gauge invariant Yukawa sector of the third fermionic generation and family universality in the first two while not allowing coupling between Z' and light neutrinos.

The neutral current interactions of this additional vector boson with the SM fermions are given as

$$\mathcal{L}^{Z'}_{\mathrm{NC}} = -\sum_f \bar{\psi}_f \gamma^\mu (C_{f,L} P_L + C_{f,R} P_R) \psi_f Z'_\mu, \tag{5}$$

where left- (L) and right- (R) handed coefficients are written as

$$\begin{aligned} C_{f,L} &= -g_Z \sin\theta' \,(T^3_f - \sin^2\theta_W Q_f) + (\tilde{g} Y_{f,L} + g' z_{f,L}) \cos\theta', \\ C_{f,R} &= g_Z \sin^2(\theta_W) \sin(\theta') Q_f + (\tilde{g} Y_{f,R} + g' z_{f,R}) \cos(\theta'). \end{aligned} \tag{6}$$

The parameters given in these expressions can be found in Ref. [18].

The contribution of this Z' gauge boson to the AMMs of the charged leptons a_f, for $f = e, \mu, \tau$ is given by [19]

$$\begin{aligned} \Delta a_f = \frac{m_f^2}{4\pi^2 m_{Z'}^2} \Bigg(& C_{f,V}^2 \int_0^1 \frac{x^2(1-x)}{1 - x + x^2 m_\alpha^2 / m_{Z'}^2} dx \\ & - C_{f,A}^2 \int_0^1 \frac{x(1-x)(4-x) + 2x^3 m_f^2 / m_{Z'}^2}{1 - x + x^2 m_f^2 / m_{Z'}^2} dx \Bigg), \end{aligned} \tag{7}$$

where $C_{f,V} = \frac{C_{f,R} + C_{f,L}}{2}$ and $C_{f,A} = \frac{C_{f,R} - C_{f,L}}{2}$. For the limits $m_f \ll m_{Z'}$ and $m_f \gg m_{Z'}$, Eq. (7) reduces to [9]

$$\Delta a_f \simeq \begin{cases} m_f^2 (C_{f,V}^2 - 5 C_{f,A}^2)/(12\pi^2 m_{Z'}^2), & m_f \ll m_{Z'}, \\ (m_{Z'}^2 C_{f,V}^2 - 2 m_f^2 C_{f,A}^2)/(8\pi^2 m_{Z'}^2), & m_f \gg m_{Z'}. \end{cases} \tag{8}$$

It is important to note that the contribution of the Z' to the AMMs of leptons is primarily determined by their vector and axial couplings which are expressed in Eq. (6), as well as the mass of the Z' boson. Using the charge assignments in Ref. [18], one can find the contributions to AMMs of electron and muon as

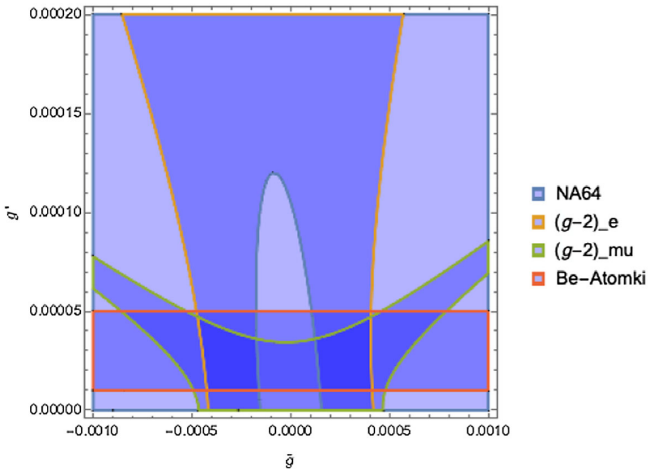

FIG. 1. Allowed parameter space mapped on the $(g', \tilde{g})$ plane for Z' mass of 17 MeV against four different experimental constraints.

$$\begin{aligned} \Delta a_e &= -3.6x10^{-6} g'^2 + 6.5x10^{-6} g'\tilde{g} + 4.6x10^{-6} \tilde{g}^2, \\ \Delta a_\mu &= -0.99 g'^2 + 0.00775 g'\tilde{g} + 0.00543 \tilde{g}^2. \end{aligned} \tag{9}$$

Furthermore, the vector and axial couplings of the quarks are important in explaining the Atomki anomaly via the transition.^{8}Be$^* \to {}^8$Be Z' [20]. In particular, the contribution of the quark axial couplings $C_{q,A}$ in this transition is greater than that of the vector couplings $C_{q,V}$ because the $C_{q,A}$ and $C_{q,V}$ terms are proportional to $k/M_{Z'}$ and $k^3/M^3_{Z'}$ (where k is the small momentum of the Z'), respectively [21]. According to $U(1)'$ charges in the model, $|C_{q,A}|$ equals to g'.

II. COMPUTATIONAL SETUP AND EXPERIMENTAL CONSTRAINTS

In our numerical analysis, we have employed SPheno 4.0.4 [22–24] generated with SARAH 4.14.3 [25,26]. In Fig. 1, we show the portion of $(g', \tilde{g})$ parameter space that satisfies the current experimental bounds from $(g-2)_{e,\mu}$, the ^{8}Be* anomaly and NA64 (as well as electron beam dump experiments) [27–30]. Here, the darkest shaded blue regions comply with all such constraints. Considering the similar plot in Ref. [18], one can see that the allowed regions have changed slightly. During the scanning of the $U(1)'$ parameter space, within the ranges specified in Table I, the Metropolis-Hastings algorithm has been used.

TABLE I. Scanned parameter space of our model.

Parameter	Scanned range	Parameter	Scanned range
g'	$[10^{-5}, 5\times10^{-5}]$	λ	[0.132, 0.125]
$\tilde{g}$	$[-10^{-3}, 10^{-3}]$	λ_χ	$[10^{-5}, 10^{-3}]$
v_S	[0.1, 1] TeV	κ	$[10^{-6}, 10^{-3}]$

After data collection, we implement Higgs boson mass bounds [31,32] as well as constraints from branching ratios (BRs) of B decays such as $\mathrm{BR}(B \to X_s\gamma)$ [33], $\mathrm{BR}(B_s \to \mu^+\mu^-)$ [34], and $\mathrm{BR}(B_u \to \tau\nu_\tau)$ [35]. We have also bounded the Z/Z' mixing to be less than a few times 10^{-3} as a result of electroweak precision tests [36].

The experimental constraints can be summarized as follows:

$$\begin{aligned} m_h &= 122\text{–}128\ \mathrm{GeV}\ \text{(as our masses are lowest order)},\\ 2.99\times10^{-4} \le \mathrm{BR}(B \to X_s\gamma) &\le 3.87\times10^{-4}\ (2\sigma\ \text{tolerance}),\\ 0.15 \le \frac{\mathrm{BR}(B_u \to \tau\nu_\tau)}{\mathrm{BR}(B_u \to \tau\nu_\tau)_{\mathrm{SM}}} &\le 2.41\ (3\sigma\ \text{tolerance}),\\ \Delta a_e &= (4.8 \pm 9.0)\times10^{-13}\ (3\sigma\ \text{tolerance}),\\ \Delta a_\mu &= (2.51 \pm 1.77)\times10^{-9}\ (3\sigma\ \text{tolerance}). \end{aligned} \tag{10}$$

Additionally, the cross section values for the given processes at the LHC have been calculated by using CalcHEP/MadGraph5 [37,38].

III. RESULTS

A. Constraints on parameter space

In this section, we will first present the dependence of Δa_μ and Δa_e upon the fundamental parameters g' and $\tilde{g}$. Figure 2 depicts Δa_μ vs Δa_e with different color bars that show g' (top panel) and $\tilde{g}$ (bottom panel). Herein, considering Eq. (9), one can learn about the favored $(g', \tilde{g})$ space in order to obtain AMMs for each 1σ, 2σ, and 3σ value. Additionally to Fig. 1, the panels in this figure give us significant information about how the different slices of parameter space are correlated to the AMMs. As seen from the plots, the experimental bounds of Δa_μ and Δa_e within 3σ allow for a narrow range in $\tilde{g}$, namely, $-0.6\times10^{-3} \lesssim \tilde{g} \lesssim -0.4\times10^{-3}$ while g' lies in the range of $0.2\times10^{-4} \lesssim g' \lesssim 0.5\times10^{-4}$. It is important to note that each area between the AMMs contours covers varied regions of the $(g', \tilde{g})$ plane within these bounds.

Now, let us focus on Z' properties, such as its mass $m_{Z'}$ and proper lifetime $c\tau$. In the top panel of Fig. 3, we demonstrate how Z' mass solutions showed in the color bar correlate with Δa_μ and Δa_e. Herein, our 1σ solutions are excluded for $m'_Z \approx 17$ MeV, the best value satisfying the Atomki anomaly. This exclusion mainly arises from the tension between the AMMs and m'_Z. As can be seen from Eq. (9), g' provides significant contributions to Δa_μ and Δa_e while it also impacts the Z' mass since $m_{Z'} = g' z_\chi v'$. Therefore, such a Z' mass value to fit the Atomki anomaly puts a limit on g' when it is located out of the 1σ region as shown in the top panel of Fig. 2. We also examine the Z' lifetime since it is crucial to explore potentially displaced signatures at the LHC. The plot at the bottom of Fig. 3 showcases the proper lifetime of Z' in milimeters over the mass range 16.7 MeV $\lesssim m'_Z \lesssim$ 18 MeV while the color bar indicates $\tilde{g}$. As mentioned in Ref. [39], for small values of $|\tilde{g}|$, the Z' lifetime becomes longer. Considering the $\tilde{g}$ solutions which fulfill all experimental conditions, the lifetime of the Z' should be $\sim10^{-3}$ mm, which is not sufficient to produce a displaced detector signal.

B. Z' production at the LHC

Now, we will study the collider signatures of our light Z' boson in three different channels at the LHC: Drell-Yan (DY) and Z' pair production through both SM-like Higgs h_2 and exotic Higgs h_1 mediation, wherein we consider both fully leptonic and semileptonic final states.

1. Drell-Yan

At the LHC, the most favored process for a light Z' boson is the DY channel, where it can directly be generated via $q\bar{q}$ fusion in s-channel. In Fig. 4, we present the dilepton production cross section via our light Z' resonance. Although the corresponding Z' production and decay rates are always large for $m_{Z'} \approx 17$ MeV, the process is difficult to detect given the very light Z', implying very soft decay products. Hence, our Z' is not really constrained by present LHC data, so that all points presented in this plot (at $\sqrt{s} = 14$ TeV) are amenable to experimental investigation during Run 3. However, a more striking signature would be Z' pair production, to which we turn next.

2. Z' pair production via SM-like Higgs mediation

As $m_{Z'} \ll m_{h_{1,2}}/2$, our light Z' boson can be pair produced via both Higgs bosons h_1 and h_2. Let us start with SM-like Higgs mediation. In Fig. 5, we present the cross section of the ensuing four-lepton final state at $\sqrt{s} =$ 14 TeV for the solutions satisfy all experimental bounds considered so far, with the additional requirement $\mathrm{BR}(h_2 \to Z'Z' \to 4l) < 5\times10^{-6}$, following ATLAS [40] and CMS [41] results. The color bar shows the mass of the Z' while the dashed line shows the SM cross section for $pp \to 4l$, $\sigma_{\mathrm{SM}} \approx 0.5$ fb, for the mass region 120 GeV $\le m_{4l} \le$ 130 GeV. As can be seen, the rates for

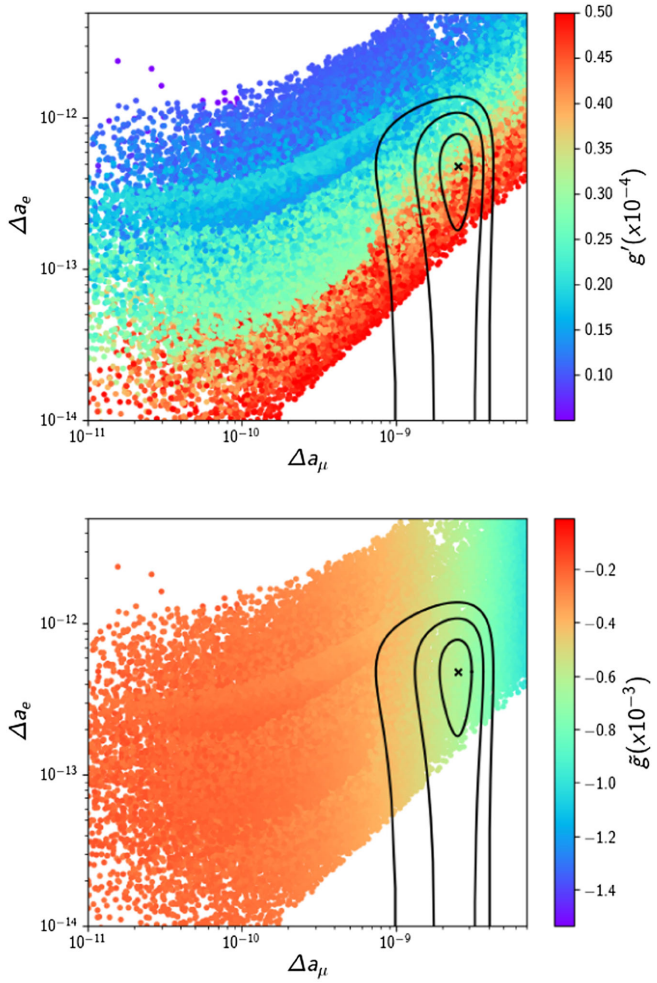

FIG. 2. Results for g' (top) and $\tilde{g}$ (bottom) in terms of $(g-2)_e$ vs $(g-2)_\mu$. Each solid line from inner to outer represents 1σ, 2σ, and 3σ bounds from the experimental central values in Eq. (10).

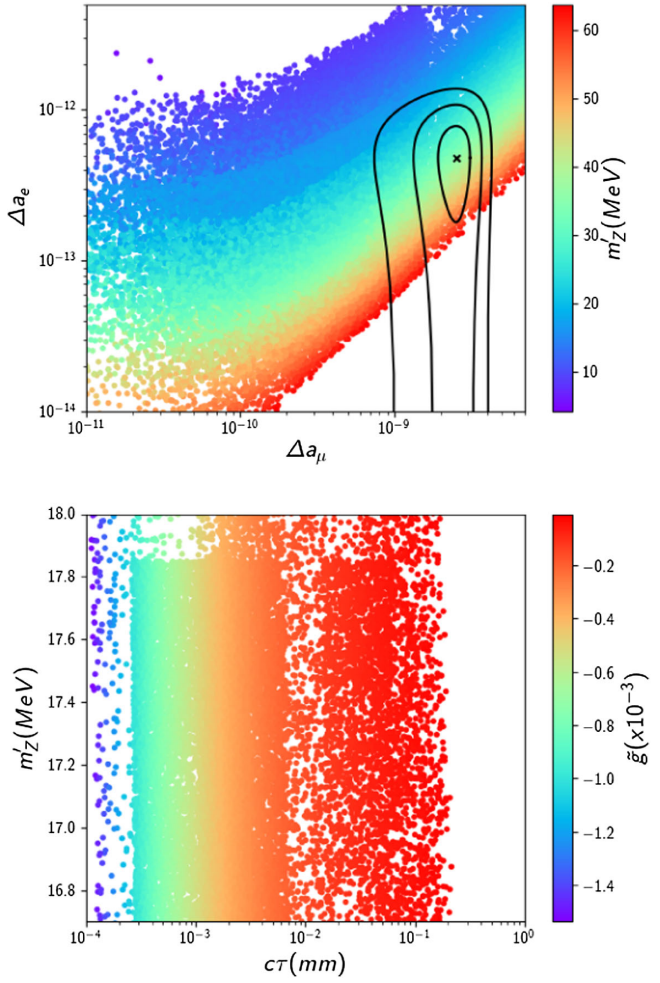

FIG. 3. Results for $m_{Z'}$ in terms of $(g-2)_e$ vs $(g-2)_\mu$ (top) and for $\tilde{g}$ in terms of $m_{Z'}$ vs the proper lifetime of the Z' (for $m'_Z \approx 17$ MeV).

$\sigma(pp \to h_2 \to Z'Z' \to 4l)$ can be rather large, up to ≈ 0.1 fb, over a wide range of m_{h_1}, including very small values of the latter, which in turn call for studying h_1 mediation, in our next section. Considering the solutions with 0.1 fb cross sections without any cuts, in order to get an excess with 3σ significance $(S/\sqrt{B})$ in the mass region $m_{4l} \approx 125$ GeV in run 3, it is needed to gather data corresponding integrated luminosity of 500 fb^{-1}, at least.

3. Z' pair production via exotic Higgs mediation

In this final part, we investigate Z' pair production via the new exotic Higgs, h_1. Figure 6 shows $\sigma(pp \to h_1 \to Z'Z' \to 4l)$ correlated to m_{h_1} as well as $m_{Z'}$, for the same parameter space considered in the previous plot (again, $\sqrt{s} = 14$ TeV). In this case, the four-lepton rate can be larger than 10×10^{-3} pb for a light h_1 while reaching 2×10^{-5} pb for m_{h_1} tending to m_{h_2}. Black and red lines show the SM differential cross sections for $\sqrt{s} = 14$ TeV,

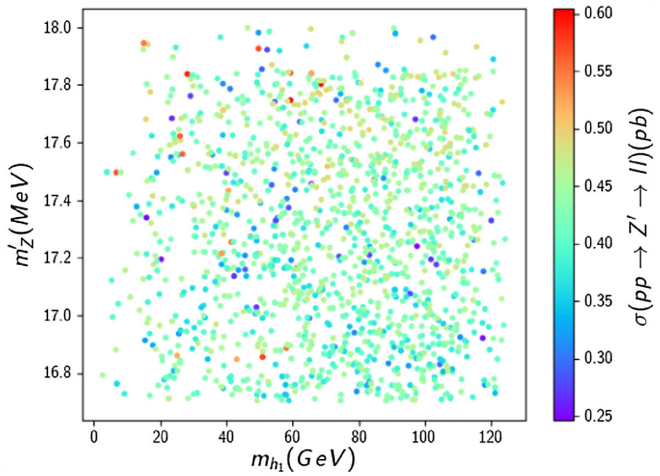

FIG. 4. Results for $\sigma(pp \to Z' \to ll)$ $(l = e, \mu)$ in terms of m_{h_1} vs $m_{Z'}$, for $\sqrt{s} = 14$ TeV.

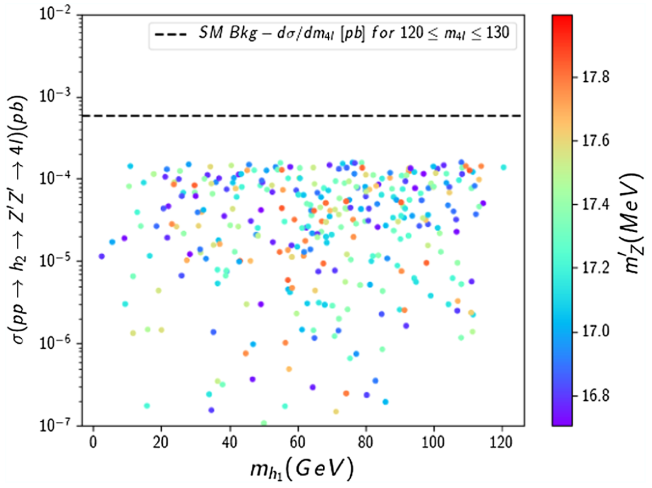

FIG. 5. Results for $m_{Z'}$ in terms of m_{h_1} vs $\sigma(pp \to h_2 \to Z'Z' \to 4l)$, for $\sqrt{s} = 14$ TeV. The dashed line shows the SM cross section of $pp \to 4l$ for the mass region of $120 \leq m_{4l} \leq 130$.

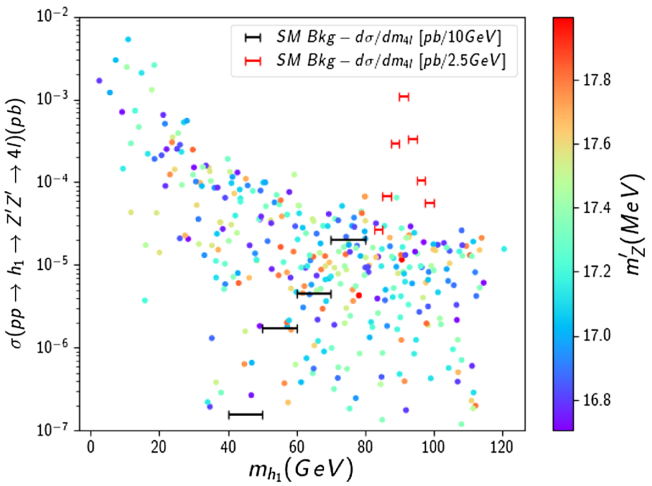

FIG. 6. Results for $m_{Z'}$ in terms of m_{h_1} vs $\sigma(pp \to h_1 \to Z'Z' \to 4l)$, for $\sqrt{s} = 14$ TeV. Black and red lines show the SM differential cross sections as a function of four lepton invariant mass with 10 and 2.5 GeV bin size, respectively.

calculated by MadGraph [42], as a function of the four-lepton invariant mass with 10 and 2.5 GeV bin size, respectively. We especially use 2.5 GeV bin size for the mass region $m_{h_1} \geq 80$ GeV, where the SM background is dominant. Similar results for the SM differential cross sections for the four-lepton final state at $\sqrt{s} = 13$ TeV were published by the ATLAS collaboration in Fig. 5 of Ref. [43]. As seen from the figure, for $m_{h_1} \leq 85$ GeV, we have many solutions giving a clear signal around $m_{4l} \approx m_{h_1}$ in the four-lepton invariant mass distribution due to a small SM background. The mass region 85 GeV $\leq m_{h_1} \leq 95$ GeV is instead challenging since the $q\bar{q} \to Z \to 4l$ channel is dominant. We also have a small window in the mass region of 95 GeV $\leq m_{h_1} \leq 100$ GeV. Considering the solutions with largest cross sections, $\sigma \approx 0.01$ fb without any cuts, it is possible to obtain an excess with 2.5σ significance using data corresponding to an integrated luminosity of 3000 fb^{-1}. Herein, in order to reduce this background, it is possible to use invariant mass cuts for leading and/or subleading lepton pairs. Hence, the h_1 mediated process, depending on the m_{h_1} value, producing a Z' pair decaying into four-lepton final states, can actually be the best way to access both the new Higgs and new gauge sectors of our scenario.

IV. CONCLUSION

In summary, a rather simple theoretical framework (assuming a nonuniversally coupled (to fermions) Z' boson, with a mass of $O(10)$ MeV, emerging from a spontaneously broken $U(1)'$ group additional to the SM gauge symmetries) is able to explain several data anomalies currently existing at low energies while predicting a clear signal at high energies. Namely, the latter is a very clean process, potentially extractable at the upcoming run 3 of the LHC, i.e., $pp \to h_i \to Z'Z' \to 4l$ ($l = e, \mu$), where h_1 and h_2 are the new Higgs state associated to the additional gauge group and the SM-like one already discovered, respectively. Hence, a new "golden channel" involving again four leptons in the final state could soon give access to both a new neutral Higgs and gauge boson.

ACKNOWLEDGMENTS

S. K. is partially supported by the Science, Technology and Innovation Funding Authority (STDF) under Grant No. 37272. S. M. is supported in part through the New connections between Experiment and Theory (NExT) Institute and the Science and Technology Facilities Council (STFC) Consolidated Grant No. ST/L000296/1. The work of Y. H. is supported by The Scientific and Technological Research Council of Turkey (TUBITAK) in the framework of the 2219-International Postdoctoral Research Fellowship Programme and by Balikesir University Scientific Research Projects with Grant No. BAP-2022/083.

[1] J. Gulyás, T. J. Ketel, A. J. Krasznahorkay, M. Csatlós, L. Csige, Z. Gácsi, M. Hunyadi, A. Krasznahorkay, A. Vitéz, and T. G. Tornyi, Nucl. Instrum. Methods Phys. Res., Sect. A **808**, 21 (2016).
[2] A. J. Krasznahorkay, M. Csatlós, L. Csige, Z. Gácsi, J. Gulyás, M. Hunyadi, T. J. Ketel, A. Krasznahorkay, I. Kuti, B. M. Nyakó *et al.*, Phys. Rev. Lett. **116**, 042501 (2016).
[3] N. J. Sas, A. J. Krasznahorkay, M. Csatlós, J. Gulyás, B. Kertész, A. Krasznahorkay, J. Molnár, I. Rajta, J. Timár, I. Vajda *et al.*, arXiv:2205.07744.
[4] A. J. Krasznahorkay, M. Csatlós, L. Csige, J. Gulyás, T. J. Ketel, A. Krasznahorkay, I. Kuti, Á. Nagy, B. M. Nyakó, N. Sas *et al.*, EPJ Web Conf. **142**, 01019 (2017).
[5] A. J. Krasznahorkay, M. Csatlós, L. Csige, J. Gulyás, M. Hunyadi, T. J. Ketel, A. Krasznahorkay, I. Kuti, Á. Nagy, B. M. Nyakó *et al.*, Proc. Sci. BORMIO2017 (**2017**) 036, https://pos.sissa.it/302/036/pdf.
[6] A. J. Krasznahorkay, M. Csatlós, L. Csige, J. Gulyás, M. Hunyadi, T. J. Ketel, A. Krasznahorkay, I. Kuti, Á. Nagy, B. M. Nyakó *et al.*, EPJ Web Conf. **137**, 08010 (2017).
[7] A. J. Krasznahorkay, M. Csatlós, L. Csige, Z. Gácsi, J. Gulyás, Á. Nagy, N. Sas, J. Timár, T. G. Tornyi, I. Vajda *et al.*, J. Phys. Conf. Ser. **1056**, 012028 (2018).
[8] B. Barman, P. Ghosh, A. Ghoshal, and L. Mukherjee, J. Cosmol. Astropart. Phys. 08 (2022) 049.
[9] A. Bodas, R. Coy, and S. J. D. King, Eur. Phys. J. C **81**, 1065 (2021).
[10] P. Fayet, Phys. Rev. D **103**, 035034 (2021).
[11] T. Nomura and P. Sanyal, J. High Energy Phys. 05 (2021) 232.
[12] O. Seto and T. Shimomura, J. High Energy Phys. 04 (2021) 025.
[13] C. Hati, J. Kriewald, J. Orloff, and A. M. Teixeira, J. High Energy Phys. 07 (2020) 235.
[14] B. Puliçe, Chin. J. Phys. (Taipei) **71**, 506 (2021).
[15] L. Delle Rose, S. Khalil, and S. Moretti, Phys. Rev. D **96**, 115024 (2017).
[16] J. L. Feng, B. Fornal, I. Galon, S. Gardner, J. Smolinsky, T. M. P. Tait, and P. Tanedo, Phys. Rev. D **95**, 035017 (2017).
[17] P. H. Gu and X. G. He, Nucl. Phys. **B919**, 209 (2017).
[18] L. Delle Rose, S. Khalil, S. J. D. King, S. Moretti, and A. M. Thabt, Phys. Rev. D **99**, 055022 (2019).
[19] J. P. Leveille, Nucl. Phys. **B137**, 63 (1978).
[20] J. Kozaczuk, D. E. Morrissey, and S. R. Stroberg, Phys. Rev. D **95**, 115024 (2017).
[21] J. L. Feng, B. Fornal, I. Galon, S. Gardner, J. Smolinsky, T. M. P. Tait, and P. Tanedo, Phys. Rev. Lett. **117**, 071803 (2016).
[22] W. Porod, Comput. Phys. Commun. **153**, 275 (2003).
[23] W. Porod and F. Staub, Comput. Phys. Commun. **183**, 2458 (2012).
[24] J. Braathen, M. D. Goodsell, and F. Staub, Eur. Phys. J. C **77**, 757 (2017).
[25] F. Staub, Comput. Phys. Commun. **185**, 1773 (2014).
[26] F. Staub, Adv. High Energy Phys. **2015**, 840780 (2015).
[27] H. Davoudiasl and W. J. Marciano, Phys. Rev. D **98**, 075011 (2018).
[28] L. Morel, Z. Yao, P. Cladé, and S. Guellati-Khélifa, Nature (London) **588**, 61 (2020).
[29] B. Abi *et al.* (Muon $g-2$ Collaboration), Phys. Rev. Lett. **126**, 141801 (2021).
[30] D. Banerjee *et al.* (NA64 Collaboration), Phys. Rev. D **101**, 071101 (2020).
[31] S. Chatrchyan *et al.* (CMS Collaboration), Phys. Lett. B **716**, 30 (2012).
[32] G. Aad *et al.* (ATLAS Collaboration), Phys. Lett. B **716**, 1 (2012).
[33] Y. Amhis *et al.* (HFLAV Collaboration), arXiv:1207.1158.
[34] R. Aaij *et al.* (LHCb Collaboration), Phys. Rev. Lett. **110**, 021801 (2013).
[35] D. Asner *et al.* (HFLAV Collaboration), arXiv:1010.1589.
[36] J. Erler, P. Langacker, S. Munir, and E. Rojas, J. High Energy Phys. 08 (2009) 017.
[37] A. Belyaev, N. D. Christensen, and A. Pukhov, Comput. Phys. Commun. **184**, 1729 (2013).
[38] J. Alwall, R. Frederix, S. Frixione, V. Hirschi, F. Maltoni, O. Mattelaer, H. S. Shao, T. Stelzer, P. Torrielli, and M. Zaro, J. High Energy Phys. 07 (2014) 079.
[39] T. Lagouri, Phys. Scr. **97**, 024001 (2022).
[40] G. Aad *et al.* (ATLAS Collaboration), J. High Energy Phys. 03 (2022) 041.
[41] A. Tumasyan *et al.* (CMS Collaboration), Eur. Phys. J. C **82**, 290 (2022).
[42] T. Stelzer and W. F. Long, Comput. Phys. Commun. **81**, 357 (1994).
[43] G. Aad *et al.* (ATLAS Collaboration), J. High Energy Phys. 07 (2021) 005.